This article has been accepted for publication in a future proceedings of this conference, but has not been fully edited. Content may change prior to final publication.
Citation information: DOI: 10.1109/CPERE65146.2025.11240009, 2025 IEEE Conference on Power Electronics and Renewable Energy (CPERE)

Transient Stability Analysis and Optimal Control Strategy of Grid-Forming Converters Based on Circular Current Limiter

Kunqi Han
School of Electrical and Power Engineering
Hohai University
Nanjing, China
hkq_hhu@hhu.edu.cn

Qiang Qian
School of Electrical and Power Engineering
Hohai University
Nanjing, China
qianqiang@hhu.edu.cn

Li Zhang
School of Electrical and Power Engineering
Hohai University
Nanjing, China
zhanglinuaa@hhu.edu.cn

Ahmed F. Zobaa
College of Engineering, Design and Physical Sciences
Brunel University of London
Uxbridge, U.K.
azobaa@ieee.org

Sobhy Mohamed Abdelkader
Department of Electrical Power Engineering
Egypt-Japan University of Science and Technology
New Borg El-Arab, Egypt
sobhy.abdelkader@ejust.edu.eg

Diaa-Eldin A. Mansour
Department of Electrical Power Engineering
Egypt-Japan University of Science and Technology
New Borg El-Arab, Egypt
diaa.mansour@ejust.edu.eg

***Abstract*—To limit transient current overshoot in grid-forming (GFM) converters caused by grid voltage sags, a variety of current limiting strategies, including priority-based limiter and circular current limiter (CCL) are employed. Existing research predominantly focuses on the transient stability analysis of priority-based limiting strategies. In this paper, an equivalent model and transient analysis method for GFM converters utilizing CCL is proposed, in which the CCL strategy is equivalent to a resistor inserted in series within the control loop. Based on this model, transient stability analysis under current saturation conditions is further conducted by constructing power-angle curves. An optimal control strategy is proposed to enhance the system's transient stability by modifying the power references and incorporating an anti-windup loop for the integrator. Finally, simulation results verify the effectiveness of the proposed transient stability analysis method and the optimized control strategy.**

Keywords—Grid-forming Converter, Transient Stability, Virtual Synchronous Generator, Circular Current Limitation, Integration Saturation

I. INTRODUCTION

The power system of China is currently transitioning towards a new power system architecture dominated by renewable energy sources. This transition has led to increasingly prominent issues of low system inertia and weak damping [1], which greatly weaken the system's anti-interference ability, deteriorate the system's frequency stability, and seriously threatens the safe and stable operation. Meanwhile, the Virtual Synchronous Generator (VSG) control for GFM converters is recognized as a reliable solution for enhancing system inertia and damping [2].

Because the VSG system simulates the external characteristics of the synchronous machine, when the grid voltage is disturbed, the VSG system will also produce the same transient stability problem as the synchronous machine, such as short-term overcurrent [3]. Consequently, current limiting is essential to mitigate instantaneous current overshoot during faults. Existing current limiting schemes have been comprehensively reviewed in [4], among which the circular current limiter within direct limiting methods enables rapid current restriction while maintaining sinusoidal output waveforms.

Upon activation of the current limiting strategy, the GFM system undergoes a behavioral shift from a voltage source to a current source while providing grid support. Consequently, transient stability analysis under current saturation conditions becomes essential. However, existing research primarily focuses on the transient stability of systems employing priority-based current limiting methods [5]. Due to fundamental differences in current phase generation mechanisms, these analytical approaches cannot be directly applied to systems utilizing circular current limiters, resulting in relatively scarce research on transient stability for circular current limiting systems.

Moreover, regarding optimized control for enhancing transient stability, the majority of existing literature focuses on improvements to power loop control strategies [8]. In contrast, research on optimizing steady-state currents under current saturation conditions remains comparatively limited. Furthermore, most studies conducting stability analysis and optimization design tend to neglect the influence of the voltage loop integrator [10]. In practice, however, voltage loop integrator saturation significantly compromises transient stability both during current saturation and during the transition out of saturation.

Therefore, the primary contributions of this paper are summarized as follows: An equivalent circuit model for GFM systems incorporating circular current limiting is proposed. Based on this established model, transient stability analysis of the system is conducted. An optimized control scheme is developed, featuring modified power references and the addition of an integrator anti-windup loop. This scheme is specifically designed to further enhance transient stability under current saturation conditions. Finally, comprehensive

This work is supported in part by the National Key Research and Development Program of China under Grant 2024YFB2408600, in part by the by the National Natural Science Foundation of China under Grant 52322705, and in part by the special fund of Jiangsu Province for the Transformation of Scientific and Technological Achievements under Grant BA2023108.

This article has been accepted for publication in a future proceedings of this conference, but has not been fully edited. Content may change prior to final publication.
Citation information: DOI: 10.1109/CPERE65146.2025.11240009, 2025 IEEE Conference on Power Electronics and Renewable Energy (CPERE)

simulation studies validate both the proposed transient stability analysis methodology and the effectiveness of the optimized control strategy.

II. The Model of GFM Convertor System

A. System description

Fig. 1 shows the GFM converter system employing the circular current limiting strategy. The converter is connected to the three-phase grid via an LC filter comprising a filter inductor L_f and a filter capacitor C_f. The grid side is represented by an equivalent inductance L_g and an equivalent resistance R_g, with V_g denoting the grid voltage. Key system parameters are listed in Table I.

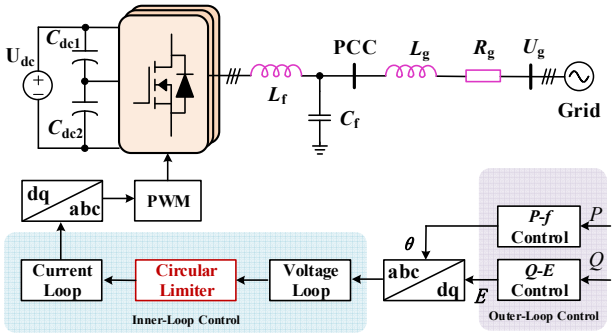

Fig. 1 GFM converter based on circular current limiting strategy

B. Control Structure

To simulate the mechanical and electrical characteristics of a conventional synchronous generator, the control scheme employs a VSG control strategy, which provides virtual damping and inertia to the system. The adopted VSG control strategy comprises the active power swing equation and the reactive power voltage equations:

The active power swing equation is given by

$$\begin{cases} T_{\text{ref}} - T_{\text{e}} - D(\omega - \omega_{\text{n}}) = J\dfrac{d(\omega - \omega_{\text{n}})}{dt} \\ T_{\text{ref}} - T_{\text{e}} = \dfrac{P_{\text{ref}} - P_{\text{e}}}{\omega} \approx \dfrac{P_{\text{ref}} - P_{\text{e}}}{\omega_{\text{n}}} \\ \dfrac{d\delta}{dt} = \omega - \omega_{\text{n}} \end{cases} \tag{1}$$

The reactive power voltage equation is given by

$$E = U_0 + k_{\text{q}}(Q_{\text{ref}} - Q_{\text{e}}) \tag{2}$$

Where J and D are the virtual inertia constant and virtual damping coefficient. θ, ω, ω_{n} denote the power angle, angular velocity, and rated angular velocity of the GFM converter system. T_{ref}, T_{e} are the torque command value and actual torque value of the converter. P_{ref}, Q_{ref}, P_{e}, Q_{e} represent the active power reference, reactive power reference, actual active power, and actual reactive power of the converter. E, U_0 are the converter voltage amplitude reference and rated value. k_{q} is the reactive power droop coefficient.

When the grid voltage drops, the converter's output voltage is unable to change instantaneously, which induces an excessive voltage difference across the filter inductor. This leads to an overcurrent in the inductor current. A current limiting strategy must be integrated into the control system to protect the converter from the impact of this abrupt current surge. Given that priority-based current limiting schemes may introduce output current distortion, this paper employs the CCL or current restriction. Its mathematical expression is given by

$$i'_{\text{dq\_ref}} \begin{cases} i_{\text{dq\_ref}} \dfrac{I_{\text{lim}}}{\sqrt{i_{\text{dref}}^2 + i_{\text{qref}}^2}} & \sqrt{i_{\text{d}}^2 + i_{\text{q}}^2} > I_{\text{lim}} \\ i_{\text{dq\_ref}} & \sqrt{i_{\text{d}}^2 + i_{\text{q}}^2} \le I_{\text{lim}} \end{cases} \tag{3}$$

Where $i'_{\text{dq\_ref}}$ is the saturated current reference. $i_{\text{dq\_ref}}$ is the original current reference generated by the voltage control loop as shown in Fig. 1. I_{lim} is the maximum allowable converter-side current magnitude. i_{dref}, i_{qref} are the d-axis and q-axis current reference components. It can be assumed that the current limiting ratio of the annular current limiter as

$$\eta = \frac{I_{\text{lim}}}{\sqrt{i_{\text{dref}}^2 + i_{\text{qref}}^2}} \tag{4}$$

III. Proposed Equivalent Circuit Model and Transient Stability Analysis

A. System Power Angle Characteristics

Assuming the converter output voltage vector is $E\angle\delta$, the grid voltage vector is $U_{\text{g}}\angle 0$. Considering the line impedance to be purely inductive in this analysis, the active power and reactive power delivered by the system can be derived as

$$\begin{cases} P_{\text{e}} = \dfrac{3EU_{\text{g}}}{2X_{\text{g}}}\sin\delta \\ Q_{\text{e}} = \dfrac{3E^2 - 3EU_g\cos\delta}{2X_g} \end{cases} \tag{5}$$

Considering the influence of the reactive power control loop, a quadratic equation with respect to the output voltage amplitude E can be derived as follows.

$$\begin{aligned} &1.5k_q E^2 + (X_g - 1.5k_q U_g\cos\delta)E - \quad \cdots \\ &(U_0 + k_q Q_m)X_g = 0 \end{aligned} \tag{6}$$

The output voltage amplitude E can be obtained as

$$\begin{aligned} E = \frac{1}{3k_q}[&1.5k_q U_g\cos\delta - X_g + \quad \cdots \\ &\sqrt{(X_g - 1.5k_q U_g\cos\delta)^2 - 6k_q X_g(U_0 + k_q Q_{\text{ref}})}] \end{aligned} \tag{7}$$

Substituting the above equation into the expression for the system output active power yields the following second-order differential equation with respect to the power angle δ

$$\begin{aligned} J\omega_n\frac{\mathrm{d}^2\delta}{\mathrm{d}t^2} + D\omega_n\frac{\mathrm{d}\delta}{\mathrm{d}t} = P_{\text{ref}} - \frac{3U_g^2}{8X_g}\sin 2\delta + \frac{U_g\sin\delta}{2k_q} - \cdots \\ \frac{U_g\sqrt{(X_g - 1.5k_q U_g\cos\delta)^2 - 6k_q X_g(U_0 + k_q Q_{\text{ref}})}}{2k_q X_g}\sin\delta \end{aligned} \tag{8}$$

Defining the state vector $\boldsymbol{x}=[x_1,x_2]^{\text{T}}=[\delta,\Delta\omega]^{\text{T}}$, and considering that the bandwidth of the power control loop is significantly lower than that of the inner voltage and current loops, the dynamic characteristics of the inner loops can be neglected. This allows us to derive the reduced-order large-signal model of the system as

This article has been accepted for publication in a future proceedings of this conference, but has not been fully edited. Content may change prior to final publication.
Citation information: DOI: 10.1109/CPERE65146.2025.11240009, 2025 IEEE Conference on Power Electronics and Renewable Energy (CPERE)

$$\begin{bmatrix}\dot{x}_1\\ \dot{x}_2\end{bmatrix}=\begin{bmatrix}x_2\\ \dfrac{P_{\mathrm{ref}}}{J\omega_n}-\dfrac{3EU_g}{2J\omega_n X_g}\sin\delta-\dfrac{Dx_2}{J\omega_n}\end{bmatrix} \tag{9}$$

When the system operates in the non-saturated current state, its behavior aligns with the established large-signal model. To analyze the transient stability, the power-angle curves under different grid voltage conditions can be plotted using equation (5), as shown in Fig. 2.

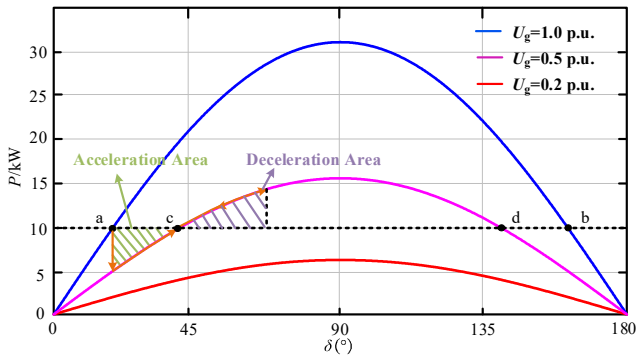

Fig. 2 System power angle curve under different voltage drop degree

From Fig. 2, it can be observed that when a grid voltage sag occurs, the system power-angle curve may have either 0 or 2 equilibrium points depending on the severity of the voltage sag. These equilibrium points refer to positions on the power-angle curve where the output power equals the reference power. For instance, when the grid voltage sags to 0.5 p.u., there exist two equilibrium points, whereas no equilibrium point exists when the voltage drops to 0.2 p.u..

When the power-angle curve has two equilibrium points, they can be respectively defined as stable equilibrium points (SEPs) and unstable equilibrium points (UEPs). For example, points a and c in Fig. 2 can be identified as SEPs, while points b and d are UEPs. According to the equal-area criterion, if the accelerating area is less than or equal to the decelerating area during a fault, the system can maintain stability at the SEP. Otherwise, it will lose stability. If no equilibrium point exists in the system, instability will occur directly. Therefore, the above analytical approach can also serve as a reference for subsequent transient stability analysis when the system enters the current-saturation state.

B. Proposed Equivalent Circuit Model

It is necessary to plot the power-angle curve under the operation to analyze the GFM system's transient stability under current saturation conditions when employing CCL. However, unlike the priority current limiting strategy, which fixes the current vector angle, the CCL uses this angle to vary with the active power loop's output. Consequently, the power-angle curve cannot be directly constructed. Therefore, this paper establishes an equivalent model of the circular current limiter to facilitate the analysis.

To facilitate transient analysis of the system loop incorporating the CCL, the following simplifications are adopted:

1. The cross-coupling effects between dq-axis components in the voltage and current control loops are neglected.

2. Given that the current control loop has significantly higher bandwidth and faster dynamics compared to the outer power loop, its transient behavior is disregarded. The output current is assumed to instantaneously track its reference, i.e., $i_{\mathrm{dq}}=i_{\mathrm{dq\_ref}}$.

3. When the system enters current saturation, it operates in current-source mode, preventing the voltage loop from regulating the output voltage to its reference. Under this condition, the voltage loop integrator accumulates errors, which could compromise system stability. Thus, the influence of the voltage loop integrator on stability is also neglected.

Based on these simplifications, the control loop can be expressed as

$$i_{\mathrm{dq\_ref}}=k_{\mathrm{vp}}\left(u_{\mathrm{dq\_ref}}-u_{\mathrm{dq}}\right)+i_{\mathrm{dq}} \tag{10}$$

Where k_{vp} is the proportional coefficient of the voltage loop. Since $i_{\mathrm{dq}}=i_{\mathrm{dq\_ref}}$, the current expression after simplification through the current limiting link can be obtained as

$$i_{\mathrm{dq}}=\eta k_{\mathrm{vp}}\left(u_{\mathrm{dq\_ref}}-u_{\mathrm{dq}}\right)+\eta i_{\mathrm{dq}} \tag{11}$$

Assuming that

$$R_{\mathrm{eq}}=\frac{1}{\eta k_{\mathrm{vp}}} \tag{12}$$

The above equation can be obtained by simplification to

$$R_{\mathrm{eq}}i_{\mathrm{dq}}=u_{\mathrm{dq\_ref}}-u_{\mathrm{dq}} \tag{13}$$

Therefore, the inner control loop with the CCL can be represented as a voltage source behind equivalent resistance R_{eq} as shown in Fig. 3.

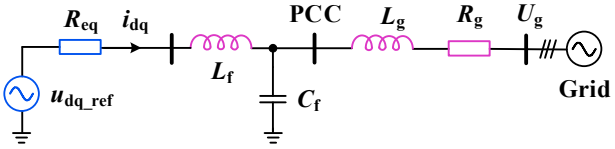

Fig. 3 Equivalent circuit of GFM converter with CCL

C. Transient Stability Analysis

In this section, the closed-loop system dynamics is derived to allow for the transient stability analysis of the converter.

Based on Fig. 3, the active power output of the system with CCL under the current saturation condition can be expressed as

$$P=\frac{3}{2}\left[\frac{R_{\mathrm{eq}}\left(E^2-EU_g\cos\delta\right)}{R_{\mathrm{eq}}^2+\omega_{\mathrm{n}}^2L_{\mathrm{g}}^2}-R_{\mathrm{eq}}I_{\mathrm{lim}}^2+\frac{\omega_{\mathrm{n}}L_{\mathrm{g}}EU_g\sin\delta}{R_{\mathrm{eq}}^2+\omega_{\mathrm{n}}^2L_{\mathrm{g}}^2}\right] \tag{14}$$

In this paper, the resistive component R_{g} can be neglected since the analysis and simulations are conducted under weak grid conditions where the grid impedance is predominantly inductive. Applying Kirchhoff's voltage law, the equivalent resistance R_{eq} of the CCL under current saturation can be derived as

$$R_{\mathrm{eq}}=\sqrt{\frac{E^2-2EU_g\cos\delta+U_{\mathrm{g}}^2}{I_{\mathrm{lim}}^2}-\omega_{\mathrm{n}}^2L_{\mathrm{g}}^2} \tag{15}$$

Therefore, the first-order closed-loop system dynamics can be represented by equations (1) and (14).

Based on the parameters listed in Table I., when the grid voltage drops to 60 % of the rated value, the power angle curves of the system both before and after entering the current

This article has been accepted for publication in a future proceedings of this conference, but has not been fully edited. Content may change prior to final publication.
Citation information: DOI: 10.1109/CPERE65146.2025.11240009, 2025 IEEE Conference on Power Electronics and Renewable Energy (CPERE)

saturation state can be calculated based on equation (14) in Fig. 4.

As observed in Fig. 4, when the grid voltage drops to 60% of its rated value, the active power reference P_{ref} persistently exceeds the system's output power P_e. Under this condition, there is no UEPs exist. According to the large-signal power-angle model established in Section III-A, when $P_{ref} > P_e$, the system maintains a positive angular velocity ω, causing continuous accumulation of the power angle δ and ultimately leading to system instability. Following this analytical framework, the transient stability of systems employing the CCL can be similarly evaluated under other grid operating conditions.

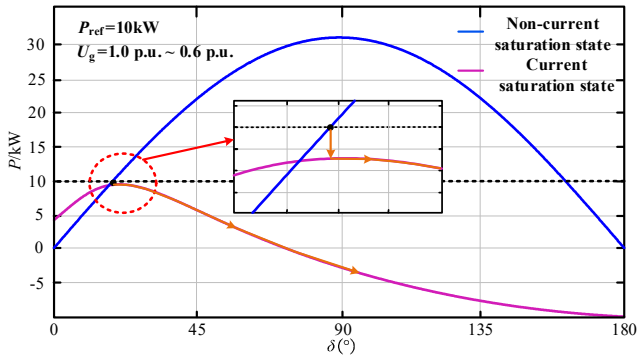

Fig. 4 Power-Angle Characteristics and Power Trajectory During Saturation Transition (u_g = 0.6 p.u., P_{ref} = 10 kW)

IV. Proposed Optimal Control Strategy

A. Power reference value adjustment

The transient stability analysis in Section II reveals that during a 60% grid voltage sag, when the system enters current saturation, the limited active power output becomes insufficient to match the normal operating power reference. This power imbalance causes continuous power angle accumulation, ultimately leading to system instability. Consequently, while the CCL successfully contains the converter current during voltage sags, its fault response characteristics require further enhancement to maintain system stability in current saturation conditions.

To solve the problem, this paper proposes an adaptive reference adjustment strategy that modifies both active and reactive power references during faults to establish SEPs for current-saturated systems. Crucially, while current limiting is fundamentally employed to mitigate transient current surges caused by the converter's inability to instantaneously adjust its output voltage during grid voltage sags, the optimal control strategy of this paper incorporates an apparent power reduction scheme proportional to the voltage sag depth. This achieves dual objectives: (1) maintaining stability through reference adaptation and (2) further reducing post-fault steady-state currents. Notably, since all considered fault scenarios involve balanced three-phase voltage sags (without negative-sequence components), the modified apparent power S_n' can be derived as

$$S_n' = \alpha_{drop} S_n \tag{16}$$

Where α_{drop} is the drop amplitude of the grid-side voltage.

To preferentially provide reactive power support to the grid during faults while reducing the active power reference, the reactive power reference is modified with priority according to different voltage sag magnitude intervals. Subsequently, the active power reference is calculated based on the modified apparent power and reactive power reference. The modified active and reactive power references according to voltage magnitude are given as

$$Q_{ref}' = \begin{cases} Q_{ref} & \alpha_{drop} > 0.9 \\ 2S_n'(1-\alpha_{drop}) & 0.5 < \alpha_{drop} < 0.9 \\ S_n' & \alpha_{drop} < 0.5 \end{cases} \tag{17}$$

$$P_{ref}' = \sqrt{(S_n')^2 - (Q_{ref}')^2} \tag{18}$$

B. Integrator anti- windup loop

The analysis in Section III-B assumes the voltage loop integrator's influence on the control system can be neglected. However, in practice, when the system enters current saturation state, the voltage loop continuously receives unidirectional error input, causing the integrator to accumulate errors persistently. After the system exits current saturation state, the saturated integrator will prevent the controller from responding promptly to input errors. Therefore, anti-windup compensation must be implemented for the voltage loop integrator.

To mitigate integrator windup, this paper enhances the existing optimized control strategy with modified power references by incorporating an anti-windup loop into the voltage-loop PI controller. The control architecture feeds back the difference between the voltage-loop output i_{dq_ref} and current-loop input i'_{dq_ref} as a positive feedback signal to the PI controller's integrator input. This introduces compensating error signals that counteract rapid unidirectional error accumulation in the PI controller, thereby preventing integrator saturation.

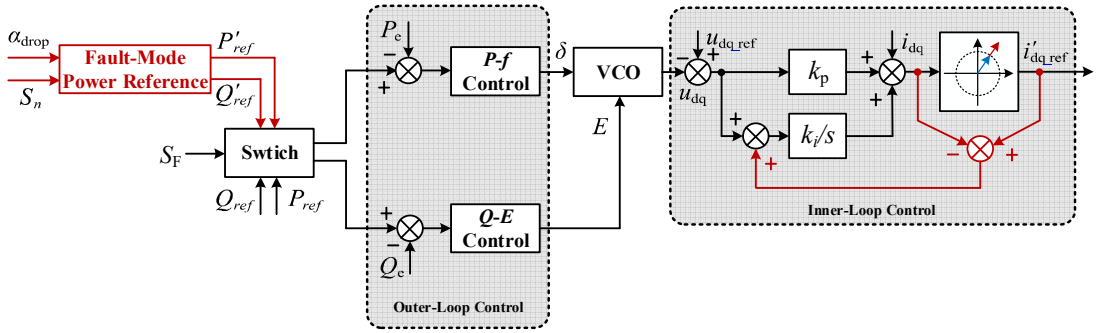

Fig. 5 The control block diagram of the proposed optimal control strategy

This article has been accepted for publication in a future proceedings of this conference, but has not been fully edited. Content may change prior to final publication.
Citation information: DOI: 10.1109/CPERE65146.2025.11240009, 2025 IEEE Conference on Power Electronics and Renewable Energy (CPERE)

Notably, the variable difference before and after the circular current limiter only exists when the limiter is active, making this approach ignored during normal operation. Compared to conventional integrator reset methods, this solution offers superior implementation feasibility within the control loop.

The control block diagram of the proposed optimized control scheme is shown in Fig. 5. The modifications introduced by the optimal control strategy of this paper, compared to conventional approaches are highlighted in red in the figure, where S_F represents the fault detection signal. When a grid voltage sag is detected, S_F is set to 1 and simultaneously triggers the activation of the optimized control scheme.

V. Simulation Results

To verify the effectiveness of the proposed optimized control scheme and transient stability analysis method, a GFM converter system employing the CCL was implemented in MATLAB/Simulink, with simulation parameters detailed in Table 1.

TABLE I. PARAMETERS OF SIMULATION MODEL

Parameter	Value
Rated Power S_n	10 kVA
Grid phase voltage u_{grms}	220 V(RMS) / 50 Hz
DC link U_{dc}	650 V
Bus Capacitance C_{dc1} C_{dc2}	1 mF
Filter inductor L_f	100 μH
Filter capacitor C_f	30 μF
Grid impedance L_g	10 mH
Switching frequency f_{sw}	24 kHz
Short-circuit ratio *SCR*	3.1
Virtual Damping *D*	6
Virtual Inertia *J*	0.1
Proportional Coefficient k_{vp}	0.6
Integral Coefficient k_{vi}	40

To verify the reliability of the transient stability analysis method presented earlier, we first conducted simulations of the system with only the circular current limiter under a 60% grid voltage sag condition. The simulation results are shown in Fig. 6.

From Fig. 6, it can be observed that the system becomes unstable after entering current saturation, and the active power curve exhibits periodic variations at a specific frequency, which is consistent with the theoretical derivation results of the transient stability analysis presented earlier.

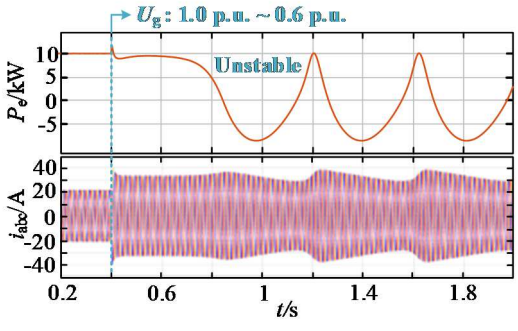

Fig. 6 Simulation result without optimal control strategy

Fig. 7(a) presents the simulation results of output active power and output current under identical operating conditions when employing the proposed optimal control strategy. The results demonstrate that the system ultimately stabilizes at SEP after entering current saturation. Fig. 7 (b) further verifies the strategy under a more severe grid voltage sag condition of 20% of rated value, showing that the system can maintain stability after regulation. These simulation results collectively validate the effectiveness of the proposed control strategy.

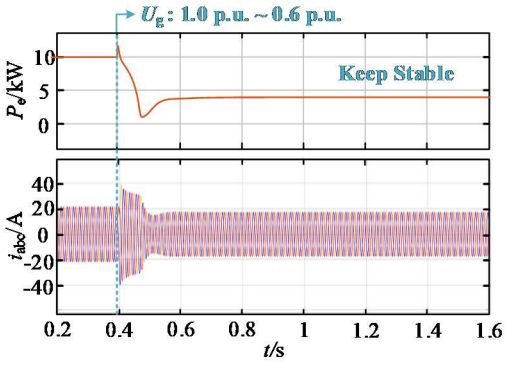

(a) The grid-side voltage drops to 60 % of the rated value

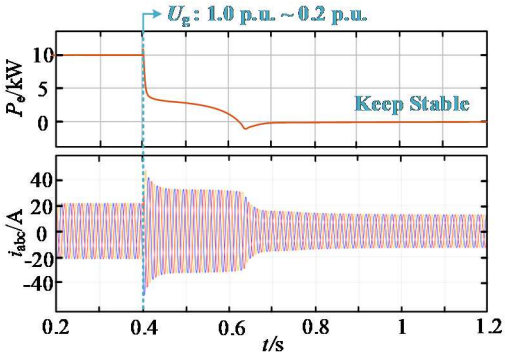

(b) The grid-side voltage drops to 20 % of the rated value

Fig. 7 Simulation result with optimal control strategy

VI. Conclusion

This paper establishes an equivalent circuit model to analyze the impact of the circular current limiter on GFM converter systems. Leveraging this model, transient stability analysis reveals that the system becomes highly susceptible to instability upon entering the current saturation state. To solve this problem, an optimized control scheme is proposed, featuring adjusted power references and the incorporation of an integrator anti-windup loop. This strategy is specifically designed to enhance the stability of GFM systems operating under current saturation conditions. Finally, the results of the simulation verify the reliability and effectiveness of both the proposed transient stability analysis method and the optimized control strategy.

References

[1] G. Lou, Q. Yang, W. Gu, J. Zhang. An improved control strategy of virtual synchronous generator under symmetrical grid voltage sag[J]. International Journal of Electrical Power & Energy Systems，2020，121：106093

[2] R. Rosso, X. Wang, M. Liserre, X. Lu, and S. Engelken, Grid-forming converters: Control approaches, grid-synchronization, and future trends— A review, IEEE Open J. Ind. Appl., vol. 2, pp. 93–109, 2021.

[3] Q. Li, P. Ge, F. Xiao, Z. Lan, Q. Ge. Study on fault ride-through method of VSG based on power angle and current flexible

regulation[J]. Proceedings of the CSEE, 2020, 40(7): 2071-2080(in Chinese)

[4] B. Fan, T. Liu, F. Zhao, H. Wu, and X. Wang, "A Review of Current-Limiting Control of Grid-Forming Inverters Under Symmetrical Disturbances," in IEEE Open Journal of Power Electronics, vol. 3, pp. 955-969, 2022,

[5] E. Rokrok, T. Qoria, A. Bruyere, B. Francois, and X. Guillaud, "Transient Stability Assessment and Enhancement of Grid-Forming Converters Embedding Current Reference Saturation as Current Limiting Strategy," in IEEE Transactions on Power Systems, vol. 37, no. 2, pp. 1519-1531, March 2022

[6] T. Liu, and X. Wang, "Transient Stability of Single-Loop Voltage-Magnitude Controlled Grid-Forming Converters," in IEEE Transactions on Power Electronics, vol. 36, no. 6, pp. 6158-6162, June 2021,

[7] C. Luo, Y. Chen, S. Liao, Z. Wang, Z. Xie, and Z. Lian, "Design-Oriented Analysis and Transient Control for VSG With Current Saturation Unit," in IEEE Transactions on Power Electronics, vol. 40, no. 1, pp. 2472-2483, Jan. 2025,

[8] L. Fan. Research on transient instability mechanism and optimal control of virtual synchronous generator considering current saturation effect[D]. Huazhong University of Science and Technology, 2023(in Chinese)

[9] L. Huang, H. Xin, Z. Wang, L. Zhang, K. Wu, and J. Hu, "Transient Stability Analysis and Control Design of Droop-Controlled Voltage Source Converters Considering Current Limitation," in IEEE Transactions on Smart Grid, vol. 10, no. 1, pp. 578-591, Jan. 2019

[10] W. Yang, C. Tu, X. Fan, and Q. Guo. A VSG transient stability enhancement method for improving frequency stability [J]. *Proceedings of the CSEE*, 2025, 45(01): 52-66. (in Chinese)